Publishing House
AKAPIT

COMPUTER METHODS IN MATERIALS SCIENCE

Informatyka w Technologii Materiałów

Vol. 13, 2013, No. 3

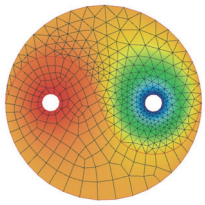

FLOW STRESS UNDER CYCLIC DEFORMATION CONDITIONS - MODELLING POSSIBILITIES*

PAULINA GRACA*, KRZYSZTOF MUSZKA, JANUSZ MAJTA

AGH University of Science and Technology, Faculty of Metals Engineering and Industrial Computer Science, Mickiewicza 30, 30-059 Kraków, Poland
**Corresponding author: graca@agh.edu.pl*

Abstract

This paper presents and discusses some aspects of the computer modelling of mechanical response of the high strength low alloy steels subjected to deformation processes where significant cyclic strain path changes exist. The proper choice of the work hardening model for the cyclic plastic deformation is essential for predicting the inhomogeneities occurring during metal forming. Aim of the current work is to discuss the differences between various hardening models with respect to their capabilities in capturing complex deformation models. Application of such models to simulate various simple plastometric tests, such as cyclic compression/tension and cyclic torsion are presented. Finally, based upon results obtained in both of the analyzed simulations, conclusions regarding the possibilities of potential application of the investigated tests in the identification process of hardening model parameters, trough the inverse analysis, are drawn.

Key words: dislocation density, combined hardening model, inverse analysis, FEM, strain path change

1. INTRODUCTION

The development of modern structural materials is closely linked with possibilities and limitations of prediction of the microstructure evolution that controls, both the physical and mechanical properties. Most of the metals forming processes are characterized by strain path changes – that are often cyclic. One of the most important phenomena in such a case is Bauschinger effect that involves reduction of the yield stress as an effect of changed loading direction.

Necessity of the use and improvement of all kind of computer modelling tools is strictly associated with progress in the materials science and manufacturing processes. In computer simulations there is a vast number of rheological models available (Szeliga et al., 2002; Lemaitre & Chaboche, 2000). Their proper choice has a significant impact on the accuracy of the results. However, majority of these models were developed based on the results of tests carried out in the idealized conditions i.e. at a constant temperature, strain rate or monotonic deformation modes. Real industrial processes however are often non-linear - characterized by constant changes in the conditions of deformation. It was found that these changes of the strain path play an important role as they significantly affect microstructure evolution and lead to different properties in the final product in comparison to monotonic modes of deformation. If this parameter is not taken into consideration at the modelling stage, it leads to a significant difference between the actual loading conditions of the process and the model, which in turn, affects the accuracy of the results.

Microalloyed steels, that are characterized by the presence of complex strengthening mechanisms are especially sensitive to changes in the strain path. It was found recently that cyclical strain reversal leads

* Paper presented during 20th KomPlasTech Conference, which was held in Zakopane, Poland on January 13-16, 2013.

 ISSN 1641-8581

to delays in both: dynamic and static recrystallization kinetics, as well as strain-induced precipitation process kinetics. It also directly affects in a similar manner austenite to ferrite phase transformation (Muszka & Majta, 2012).

The main aim of the current work is to discuss the differences between various existing hardening models with respect to their capabilities in capturing deformation behaviour during strain reversal with special focus on the possibilities of their extension in order to include microstructural factors, and thus, decreasing their empirical level. Application of such models to simulate two plastometric tests i.e. cyclic compression/tension and cyclic torsion is presented.

2. EXPERIMENT

2.1. Cyclic torsion test

Cyclic torsion test was carried out using cylindrical test specimens (with gauge diameter of 10mm and gauge length of 20 mm) that were made from S460M steel with basic chemical composition shown in table 1. The experiment was conducted at room temperature using thermomechanical simulator Arbitrary Strain Path Machine (ASP). Specimen was deformed in a cyclic manner applying forward / reverse torsion with the strain of 0.25 per pass and the strain rate of 0.1 s^{-1}. During the test, twist angle and torque were recorded and subsequently converted into equivalent plastic strain *vs* equivalent plastic strain curves using standard equations.

Table 1. *Basic chemical composition of studied steels.*

Steel	C	Si	Mn	Nb	Ti	N
S460M	0,13	0,49	1,49	0,035	0,003	0,006
L450Nb	0,075	0,292	1,61	0,0425	0,02	0,005

2.2. Cyclic tension/ compression test

Cyclic tension/compression test was performed on microalloyed steel L450Nb with basic chemical composition shown in table 1. The plastometric test was carried out using cylindrical specimen (with a strain gage diameter of 4mm and length of 12 mm) using Zwick Z250 tension/compression frame at room temperature with a strain of 0.025 per pass and the strain rate of 0.1 s^{-1}. During deformation, relative displacement as a function of force was recorded.

3. OPTIMISATION AND MODELLING RESULTS

3.1. Combined hardening model - optimization and modelling results

As it was already mentioned, the key factor for computer modelling process is selection of an appropriate rheological model. During the selection of the proper hardening model during modelling of the cyclic deformation an important aspect is to take into account the Bauschinger effect. Deformation processes characterized by a simple strain path can be modelled using an isotropic hardening model that takes into account only change in the radius of the yield surface. In most of the metal forming processes, however, material is subjected to complex strain path changes that often occur in a cyclic manner.

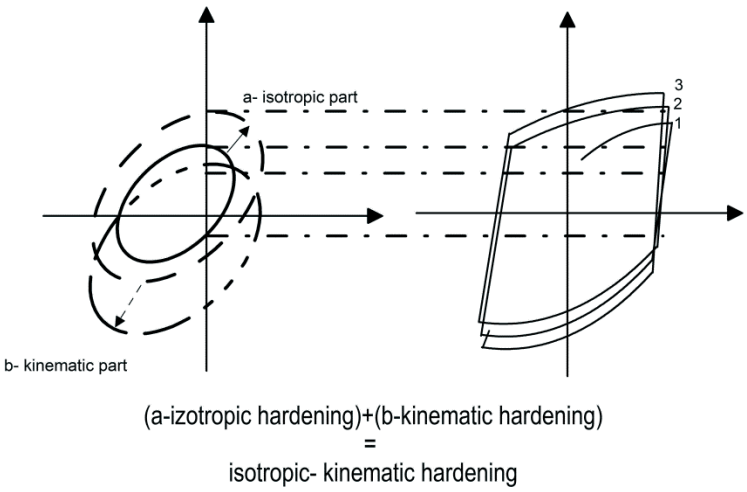

Fig. 1. *Cyclic hardening behaviour and effects of combined nonlinear hardening model parameters.*

Additionally, in the case of microalloyed steels the effects of interactions between recrystallization and precipitation kinetics as well as solid solution and precipitation strengthening make the problem especially important. In this case, there is a need for use a more complex model, which includes not only isotropic part of the hardening, but also kinematic part. During the application of the isotropic-kinematic hardening model it is possible to change

the size of the yield surface and to change its position within the stress space (see: figure 1).

In the present study two different hardening models were selected and studied with respect to their possibilities and accuracy in the modelling of cyclic deformation tests. First selected model is Chaboche model (Lemaitre & Chaboche, 2000). It's isotropic hardening component can be described by the following equation:

$$\sigma^0 = \sigma_0 + Q(1 - exp^{-b\varepsilon}) \qquad (1)$$

where: σ^0 – isotropic part of hardening; σ_0 – yield stress; Q– maximum change in yield surface b – rate of change of yield surface during plastic deformation; ε- strain. Evolution law of the kinematic part of the Chaboche hardening model is described as a sum of the backstresses, which includes parameters that control the position of the stress for each backstress:

$$\dot{\boldsymbol{\alpha}} = \frac{C_k}{\sigma^0}(\boldsymbol{\sigma} - \boldsymbol{\alpha})\varepsilon - \gamma_k \boldsymbol{\alpha}\varepsilon \qquad (2)$$

where: C_k – initial kinematic hardening modulus; γ_k – the rate at which the kinematic hardening modulus decreases with increasing plastic deformation; σ^0 – the size of the yield surface; $\boldsymbol{\sigma}$ – stress tensor; $\boldsymbol{\alpha}$ – backstress; ε – plastic strain

defines how various solutions are different from the searched one. This function sets the value of the solution error, i.e. the difference between experimental and modelling result. The schematic representation of the optimization procedure that was developed within the current work is presented on figure 2. First step of the process is to input the initial set of the model parameters as the guess values. Then FEM model of the considered process is run and a direct solution is obtained. Then, the results from the simulation are passed to the optimization module and the objective function value is calculated. Next step is evaluating the obtained values of the objective function. It is necessary to check whether the solutions obtained from the individual calculation steps are similar. If the solution meets the convergence criteria and the resulting error is satisfactory, the obtained parameters can be considered as the optimum process parameters. Otherwise, minimization process of the objective function with respect to the process parameters is performed again until the optimal solution has been found. In the case of the present work, Simplex algorithm was used as the minimization function.

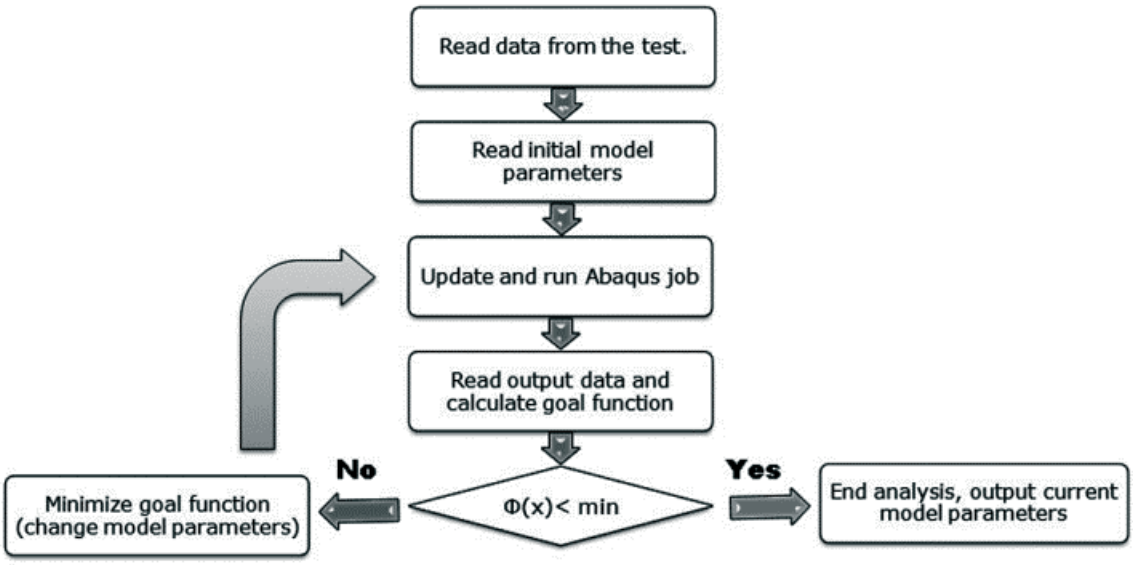

Fig. 2. *Flow chart representing optimization process using inverse method applied in the present work.*

In order to identify the parameters of the model, optimization tool utilizing inverse approach was used in the present work. Inverse analysis is one the most effective ways used to determine the coefficients of the rheological models (Szeliga et al. 2002). In this method, objective function has to be defined and used as a criterion to select acceptable solution. The current value of the objective function

In the present work, the initial parameters of the model were selected and a new direct solution for the problem was subjected to Abaqus Standard code. Finite element models of both cyclic torsion and tension/compression tests were developed and simulations of studied processes were performed. Then, the data output in the form of displacement *vs* force, or, in the case of cyclic torsion test, the twist angle

vs torque were read and compared with data obtained experimentally. The set of optimal Chaboche model parameters identified for both materials and groups tests is summarized in table 2.

Table 2. *Optimized parameters of the Chaboche model for studied tests and materials.*

Cyclic torsion test				
σ_0	Q	b	C	γ
52,9478	-0,4173	0,0163	136850,4	111,1463
Cyclic compression/ tension test				
σ_0	Q	b	C	γ
441,4	191,73	0,01069	4739	23,34

In the case of cyclic torsion tests the data obtained as rotation angle *vs* torque, were respectively converted into equivalent stress – strain curves. The comparison of the measured and calculated data for the first cycle of the forward/reverse torsion and tension-compression tests is presented in figure 3a and 3b respectively. It can be seen that application of the combined isotropic–kinematic hardening model resulted - compared with pure isotropic model - in better accuracy of the results. In the present paper, the attention was put on the first cycle of strain reversal only as proper capture of the metallurgical phenomena occurring during very first strain reversal i.e. rearrangement of dislocation substructure is a key point in understanding of the problem.

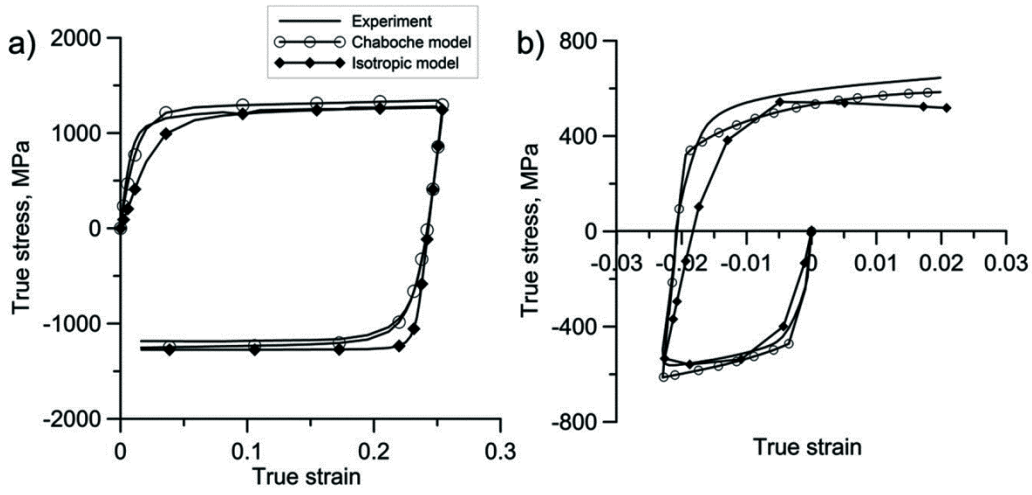

Fig. 3. *Comparison of the calculated and measured stress-strain curves recorded after first two passes of cyclic torsion test -a) and tension/compression test -b).*

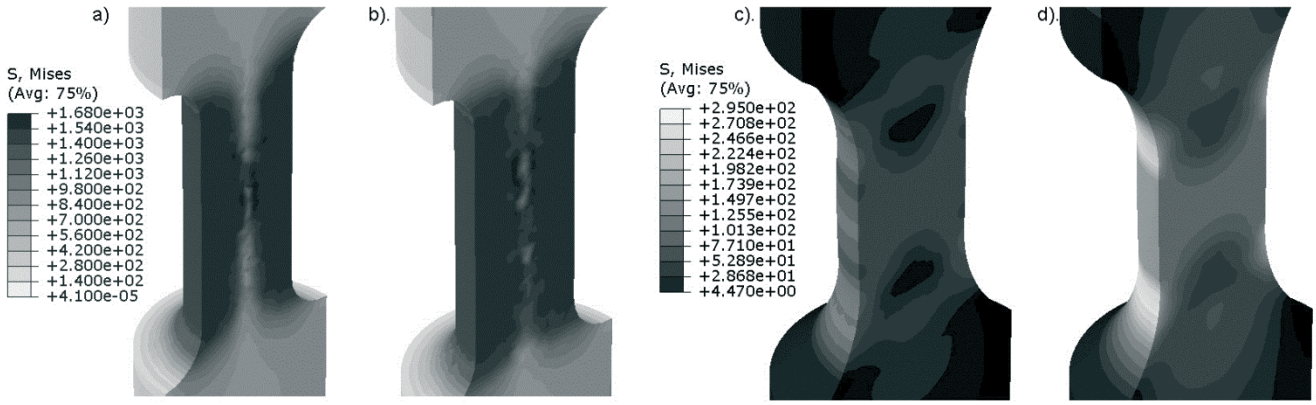

Fig. 4. Equivalent Mises stress distribution during cyclic torsion test -a), -b) and cyclic tension/compression test-c), -d). Combined isotropic-kinematic hardening model -a), -c); pure isotropic hardening model -b), -d).

This can be further seen in figure 4 where examples of equivalent Mises stress distribution maps for both considered plastometric tests are compared with the results obtained using pure isotropic hardening model. It can be noticed that, in both tests, application of combined hardening model allowed to capture more effects resulting from stress inhomogeneity, as a consequence of cyclic strain path changes, than in the case where pure isotropic hardening models were applied.

Presented results show reasonably good agreement with the experimental data obtained for various types of cyclic deformation tests. It can be seen that application of the combined hardening rule resulted in better accuracy in the prediction of the material behaviour under strain reversal. This confirms accuracy of the proposed approach. Careful choice of the proper hardening model and utilization of the inverse approach for the model parameters' identification is crucial when simulations of the strain path sensitive processes are considered.

3.2. Dislocation density-based work hardening model

In the second part of the work, different material model was selected and checked with respect to its limitations and potential of physically-based modelling of the metal forming with cyclic stain path changes. Because during strain reversal, a significant rearrangement of the dislocation substructure occurs, dislocation density as a model parameter was introduced. In the case of microalloyed steels the presence of the precipitation and solid solution strengthening mechanisms significantly affects the hardening process, also due to the retardation of dislocation substructure formation process (Sun et al., 2011). In the Chaboche model change in the size and position of the yield surface after strain path change is taken into consideration via introduction of the backstresses. However, the model parameters are purely empirical and do not have any particular physical meaning. In the following model, dislocation density is introduced and its changes upon strain reversal are reflected. General formula for the stress of the considered model is based on the Kocks model and can be shown as follows (Rauch et al, 2007):

$$\sigma = \sigma_0 + M[X + (1-\alpha)(\tau - \tau_0)] \qquad (3)$$

where: σ_0 – is the initial stress ($M\tau_0$), M- is the Taylor factor, τ_0 – is the stress related to lattice fiction and solute contents. Concerning the backstresses, an internal variable X is introduced to describe the rapid changes in stress under reverse deformation:

$$X = a(\tau - \tau_0) \qquad (4)$$

where a – fraction of the stress that experiences some delay in development of the backstress. Shear stress can be calculated from:

$$\tau = \tau_0 + \alpha G b\sqrt{\rho_f + \rho_r} \qquad (5)$$

where: G- is the shear modulus, b- the Burgers vector and α- a factor that weights the dislocation interaction. Dislocation density parameter consists of two components that are related with forward and reverse loading of dislocation substructures:

$$\frac{d\rho_f}{d\varepsilon} = \frac{1}{b\Lambda} - f\rho_f \qquad (6a)$$

$$\frac{d\rho_r}{d\varepsilon} = \frac{1}{b\Lambda} \cdot \frac{\rho_r}{\dot{\rho}_f} \qquad (6b)$$

$$\rho_f(\gamma_f = 0) = (1-p)\dot{\rho}_f \qquad (7a)$$

$$\rho_r(\gamma_f = 0) = p\dot{\rho}_f \qquad (7b)$$

During the prestrain the second component - dislocation density for reversed strain (6b) - is null and the first component (6a) accumulates following the classical evolution law in which the net dislocation storage rate is separated in two components: the athermal storage that depends on the mean free path Λ for mobile dislocations –a, and the thermally activated recovery term whose efficiency is given by the factor f that depends on the temperature and strain rate -b. After reloading, the density ρ_f increases with increasing strain as in forward loading so that its evolution is still governed (6a). By contrast, the disappearance of ρ_r, the polarized fraction of the dislocation density is captured by an additional evolutionary law that reduces to equation (6b). After the prestrain, the trapped dislocations contribute to the density $\dot{\rho}_f$. At reloading, these dislocations no longer behave like newly generated ones. Significant fraction of the substructure annihilates rapidly when the glide direction is changed. This may be understood, for example, as loops that did not expand sufficiently so that they shrink and finally collapse when the stress is inverted. To take this into consideration, it is considered that a part p of the previously stored dislocation density is sensitive to the polarity of the stress and disappears gradually when the stress sign is changed. This part is moved to ρ_r (7b). The remaining fraction of this population is trapped and supposed to behave in the same way in both directions

so that this fraction is kept in ρ_f at reloading. The splitting of the dislocation densities is then given by equations 7a and 7b. In the present study, above-mentioned model was chosen and used for an analitycal modeling of the first two passes of studied forward/reversed torsion test. Its parameters were identified using inverse optimisation tool (Solver) available in Excel. Initial dislocation density was calculated from Holt's model (Holt, 1970). Key assumption of this model is the existence of the critical distance, at which dislocations' interactions can be neglected. Then, dislocation cell size can be determined using the wavelength of the fastest growing fluctuation, which leads to the following equation:

$$d_c = k_c \rho^{-1/2} \tag{8}$$

where: d_c - size (diameter) of the dislocation cell, k_c - constant, ρ - dislocation density.

Relation between the flow stress and cell size can be derived by substituting equation (8) into the Taylor relationship:

$$d_c = \alpha k_c b \left(\frac{G}{\sigma_0}\right)^m \tag{9}$$

where: G – is the shear modulus, b – the Burgers vector, σ_0 – is the initial stress and $m = 1$.

The coefficients of applied dislocation density-based work hardening model are summarized in table 3. Based on yield stress, knowing the average dislocation cell size it is possible to rearrange the above equation and to calculate the initial dislocation density.

Figure 5 presents a comparison of measured and calculated stresses using selected models (analytical work hardening model and Chaboche model). It can be seen that the analytical solution based on dislocation density model predicts fairly well stress level-especially for higher strains. Additional advantage of this idea can be expected for forward and reverse strains as well as total dislocation density calculation, what is presented in figure 6.

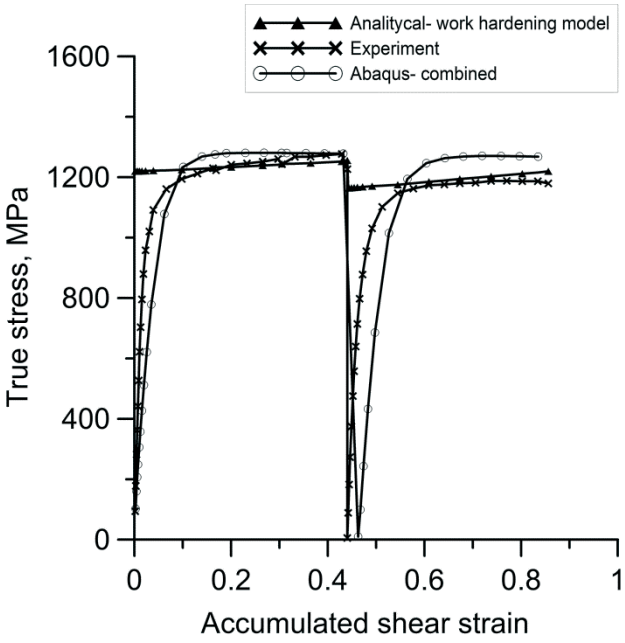

Fig. 5. *Comparison of calculated and measured stress-strain curves for studied models.*

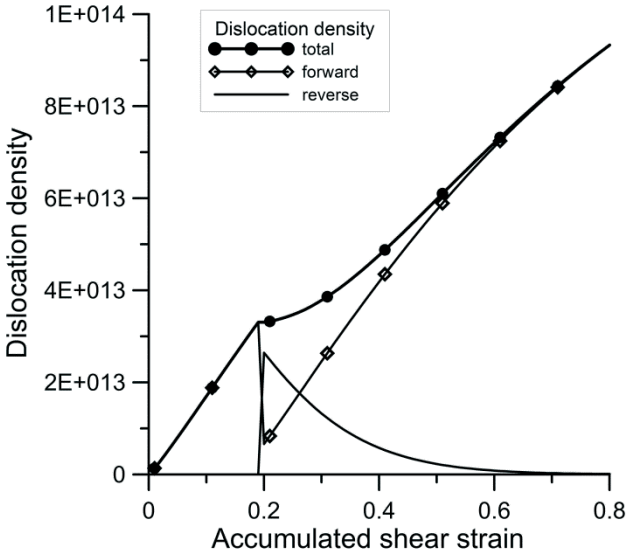

Fig. 6. *Dislocation density components for forward and reverse strains and the total dislocation density calculated using studied model.*

4. CONCLUSIONS

Based on the performed study the following conclusions can be drawn:

Table 3*. Selected values for the parameters. α is factor that weights the dislocation interactions, G is the shear modulus, b the Burgers vector, τ_o is the stress related to lattice fiction and solute contents, K is the number of forest dislocations a moving segment, D is the grain size, factor f that depends on the temperature and strain rate, C_x characterizes the dynamic of the back stresses changes, M is the Taylor factor.*

Parameters	α	G MPa	b m	τ_o MPa	K	D µm	f	p	a	M
Values	0.7	30.000	2.46×10^{-10}	120	180	30	2.8	0.8	0.6	2.8

- When a cyclic deformation process is considered, the combined hardening model should be applied in the computer simulation. The simple isotropic hardening model does not properly predict material behaviour under cyclic deformation conditions.
- Utilization of the strain path sensitive rheological model gives the possibility to use it as an universal modelling tool that takes into account deformation phenomena occurring during multiple strain reversals.
- Application of the dislocation-based hardening model for modelling of flow stress during cyclic loading shows its potential as an alternative for improvement the accuracy of mechanical behaviour compared to empirical models that are now commonly used.

ACKNOWLEDGEMENT

Financial support of Polish Ministry of Science and Higher Education (AGH grant no. 11.11.110.153) is gratefully acknowledged.

REFERENCES

Holt, D.L., 1970, Dislocation Cell Formation in Metals, *Journal of Applied Physics*, 41, 3197-3201.

Lemaitre, J., Chaboche, J., 2000, *Mechanic of solid materials*, Cambridge University Press.

Majta, J., Muszka, K., 2012, Mikrostrukturalne aspekty niejednorodności odkształcenia w modelowaniu komputerowym, *Hutnik – Wiadomości Hutnicze*, 79, 225-231.

Rauch, E.F., Gracio, J.J., Barlat, F., 2007, Work-hardening model for polycrystalline metals under strain reversal at large strains*, Acta Materialia,* 55, 2939-2948.

Sun, L., Muszka, K., Wynne, BP., Palmiere, E.J., 2011, The effect of strain path reversal on high-angle boundary formation by grain subdivision in a model austenitic steel, *Scripta Materialia*, 64, 280-283.

Szeliga, D., Matuszyk, P., Kuziak, R., Pietrzyk, M., 2002, Identification of rheological parameters on the basis of various types of plastometric tests, *Journal of Materials Processing Technology*, 125-126, 150-154

NAPRĘŻENIA UPLASTYCZNIAJĄCE W WARUNKACH ODKSZTAŁCEŃ CYKLICZNYCH- MOŻLIWOŚCI MODELOWANIA

Streszczenie

W pracy omówiono aspekty dotyczące modelowania komputerowego podczas odkształcania stali mikrostopowej o podwyższonych własnościach wytrzymałościowych przeprowadzanych z wykorzystaniem procesów charakteryzujących się zmienną ścieżką odkształcenia. Właściwy dobór modelu naprężenia uplastyczniającego do opisu zachowania się materiału podczas odkształceń cyklicznych jest niezbędny do właściwego przewidywania niejednorodności odkształcenia spowodowanej występowaniem zmiennej ścieżki odkształcania. Celem pracy jest omówienie różnic pomiędzy modelami umocnienia w odniesieniu do ich możliwości w zakresie prawidłowego odzwierciedlenia realnych procesów obejmujących zastosowanie odkształceń cyklicznych. W artykule zostało przedstawione zastosowanie tego typu modeli do symulacji prostych testów plastometrycznych, takich jak: cykliczne skręcanie próbki oraz cykliczne ściskanie/ rozciąganie próbki. Wyniki wszystkich symulacji poddano szczegółowej analizie I na tej drodze sformułowano wnioski dotyczące wykorzystania prezentowanych testów podczas identyfikacji parametrów modeli umocnienia dla odkształceń cyklicznych z wykorzystaniem analizy odwrotnej.

Received: February 18, 2013
Received in a revised form: April 23, 2013
Accepted: May 16, 2013